

Why Are Vinyl Cations Sluggish Electrophiles?

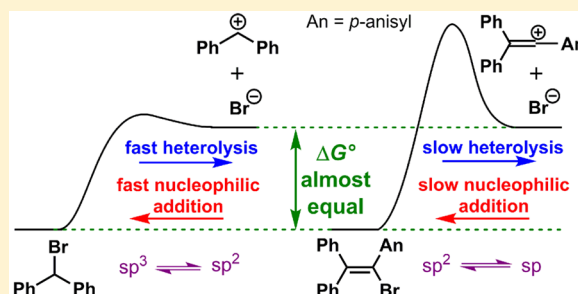
Peter A. Byrne,[†] Shinjiro Kobayashi,[†] Ernst-Ulrich Würthwein,[‡] Johannes Ammer,[†] and Herbert Mayr^{*,†}

[†]Department Chemie, Ludwig-Maximilians-Universität München, Butenandtstrasse 5-13, 81377 München, Germany

[‡]Organisch-Chemisches Institut, Westfälische Wilhelms-Universität, 48149 Münster, Germany

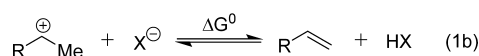
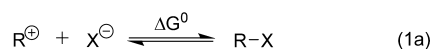
S Supporting Information

ABSTRACT: The kinetics of the reactions of the vinyl cations **2** [$\text{Ph}_2\text{C}=\text{C}^+-(4\text{-MeO-C}_6\text{H}_4)$] and **3** [$\text{Me}_2\text{C}=\text{C}^+-(4\text{-MeO-C}_6\text{H}_4)$] (generated by laser flash photolysis) with diverse nucleophiles (e.g., pyrroles, halide ions, and solvents containing variable amounts of water or alcohol) have been determined photometrically. It was found that the reactivity order of the nucleophiles toward these vinyl cations is the same as that toward diarylcarbenium ions (benzhydrylium ions). However, the reaction rates of vinyl cations are affected only half as much by variation of the nucleophiles as those of the benzhydrylium ions. For that reason, the relative reactivities of vinyl cations and benzhydrylium ions depend strongly on the nature of the nucleophiles. It is shown that vinyl cations **2** and **3** react, respectively, 227 and 14 times more slowly with trifluoroethanol than the parent benzhydrylium ion $(\text{Ph})_2\text{CH}^+$, even though in solvolysis reactions (80% aqueous ethanol at 25 °C) the vinyl bromides leading to **2** and **3** ionize much more slowly (half-lives 1.15 yrs and 33 days) than $(\text{Ph})_2\text{CH-Br}$ (half-life 23 s). The origin of this counterintuitive phenomenon was investigated by high-level MO calculations. We report that vinyl cations are not exceptionally high energy intermediates, and that high intrinsic barriers for the $\text{sp}^2 \rightleftharpoons \text{sp}$ rehybridizations account for the general phenomenon that vinyl cations are formed slowly by solvolytic cleavage of vinyl derivatives, and are also consumed slowly by reactions with nucleophiles.



INTRODUCTION

Over the course of the last century, the properties of carbocations (which frequently are reactive intermediates) have been investigated by diverse techniques to understand their role in organic chemical reactions.^{1–11} Although there exist several means for quantifying the stabilities of carbocations in solution and in the gas phase,^{2–10,12,13} general stability scales for carbocations (R^+) do not exist; that is, the absolute stability of a given carbocation cannot be uniquely defined.^{2,14} Frequently, the equilibrium constants of their reactions with a certain reference Lewis base X^- (eq 1a), that is, their Lewis



acidities with respect to X^- , are employed as a measure of their relative stabilities.^{2–9,12,15–17} Alternatively, carbocations have been ranked according to their Brønsted acidities with respect to a certain Brønsted base (eq 1b),^{2b,18} and most Brønsted acidity scales refer to the reaction medium (solvent) as the reference base.

Solvolysis reactions often proceed with rate-determining heterolytic cleavage of R-X (reverse of reaction 1a). The initially formed intermediate carbocation R^+ is then immediately trapped by the solvent and does not recombine with the leaving group.^{1,19} As the transition state of this cleavage is

generally assumed to be carbocation-like (Hammond's postulate), the rates of the solvolysis reactions of R-X have frequently been considered to be a measure for the relative stabilities of the intermediate carbocations.^{1,6c}

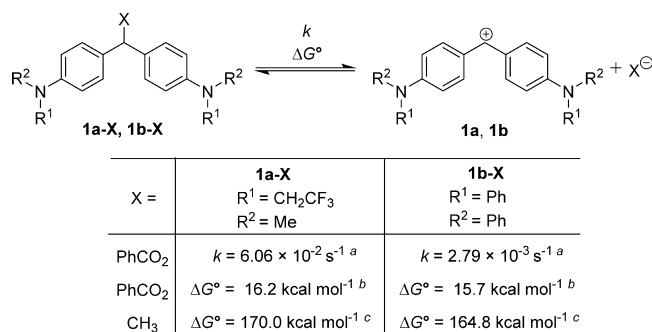
In several series of solvolysis reactions, linear relationships between the measured solvolysis rates and the Lewis acidities of the intermediate carbocations (which are derived from equilibrium measurements) have been observed, but deviations from such rate–equilibrium relationships have also been reported.^{12,15,20–22} In our investigations of the reactivities of benzhydryl derivatives, we have observed, for example, that benzhydrylium ion **1a** is formed 22 times faster than **1b** during solvolysis of the corresponding benzoates (Scheme 1)²⁰ even though **1a** is the stronger Lewis acid according to equilibrium studies in solution and computational studies for the gas phase (Scheme 1).^{12,15}

What is the origin of this discrepancy? Direct rate measurements in the solvents used for the solvolysis studies showed that most flash photolytically generated benzhydryl cations react with chloride and bromide ions under diffusion control.¹⁹ As there is obviously no barrier for the ion combination, one can conclude that in the reverse reaction (first step of an $\text{S}_{\text{N}}1$ reaction) the transition state also corresponds to the ion pair (Figure 1).

Received: October 18, 2016

Published: January 1, 2017

Scheme 1. Rate Constants (k) and Gibbs Energies of Reaction (ΔG°) for Heterolysis Reactions Giving Benzhydrylium Ions **1a and **1b****



(a) Experimental rate constant for reaction at 25 °C in 80:20 MeCN/H₂O.²⁰ (b) Gibbs reaction energy ΔG° at 20 °C calculated using $\lg K = LA + LB$,¹² in which the LA values of **1a** and **1b** in CH₂Cl₂ (−5.39 and −5.72, respectively) and the LB value of benzoate in MeCN (17.45) were employed. (c) Negative of the calculated gas-phase methyl anion affinity of the benzhydrylium ion at 20 °C (see ref 15).

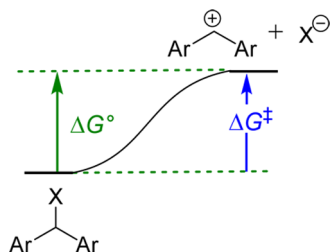


Figure 1. First step of the S_N1 reaction of a benzhydryl halide giving benzhydrylium ion and halide anion.

On the other hand, we have measured significant barriers for the combinations of benzhydrylium ions with carboxylate anions (as depicted for the reactions from right to left in Figure 2).²¹ From the principle of microscopic reversibility, one can

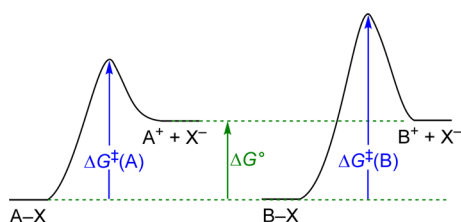


Figure 2. Comparison of ionizations of the alkyl halides A–X and B–X to give carbocations A⁺ and B⁺ of equal Lewis acidity with different rates.

now derive that the first step of an S_N1 reaction of a benzhydryl carboxylate also must proceed via a transition state that is higher in energy than the carbocation (see reactions from left to right in Figure 2).

According to Marcus (eq 2),^{23a–g} the Gibbs activation energy (ΔG^\ddagger) of a chemical reaction can be expressed by a combination of the Gibbs reaction energy (ΔG°) and the intrinsic barrier (ΔG_0^\ddagger), the latter of which corresponds to ΔG^\ddagger for an identity reaction. For reaction series where identity reactions cannot be established, for example, carbocation–anion combinations, the intrinsic barrier ΔG_0^\ddagger is commonly obtained by extrapolations to reactions with $\Delta G^\circ = 0$.^{23h}

$$\Delta G^\ddagger = \Delta G_0^\ddagger + \frac{\Delta G^\circ}{2} + \frac{(\Delta G^\circ)^2}{16\Delta G_0^\ddagger} \quad (2)$$

Consider two heterolysis reactions, involving different species A–X and B–X, that have identical Gibbs energies of reaction (ΔG°) but different Gibbs energies of activation ($\Delta G^\ddagger(A) < \Delta G^\ddagger(B)$), as shown in Figure 2. Because the thermodynamic contribution (ΔG°) to the Gibbs energy of activation in both cases is identical, the difference between $\Delta G^\ddagger(A)$ and $\Delta G^\ddagger(B)$ must arise exclusively from the differences between the intrinsic barriers $\Delta G_0^\ddagger(A)$ and $\Delta G_0^\ddagger(B)$ (not shown explicitly in Figure 2). Thus, in the case depicted in Figure 2, the intrinsic barrier $\Delta G_0^\ddagger(B)$ must be greater than $\Delta G_0^\ddagger(A)$. The energy profiles in Figure 2 now illustrate the counterintuitive conclusion that in cases where the difference of the heterolysis rates is mostly due to a difference in intrinsic barriers, the carbocation that is formed more quickly, A⁺, also reacts more quickly than B⁺ with X[−].

Let us now return to the example illustrated in Scheme 1. As the Lewis acidity of carbocation **1a** is slightly higher than that of **1b**, the higher solvolysis rate of **1a-X** as compared to **1b-X** must be due to the lower intrinsic barrier for the ionization of **1a-X** than of **1b-X**. With this conclusion, we can explain why carbocation **1a**, which is formed faster in S_N1 reactions than **1b**, has also been found to generally react faster with nucleophiles than **1b**.²⁴

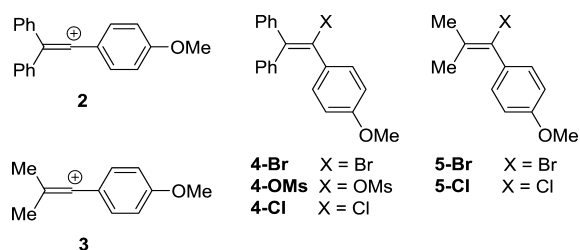
What is the consequence of these considerations for vinyl cation chemistry? The very low S_N1 reactivities of vinyl halides and vinyl tosylates^{25–27} have commonly been ascribed to low thermodynamic stabilities of vinyl cations due to the sp² hybridization of the carbenium center.^{28,29} However, when one considers that the 1-phenylvinyl cation has a hydride affinity similar to that of the benzyl cation,^{30–32} only 2.9 kcal mol^{−1} greater than that of the *tert*-butyl cation,³⁰ the question arises whether the low solvolysis rates of vinyl halides are really mostly due to the low thermodynamic stabilities of dicoordinated carbenium ions. If instead high intrinsic barriers for the sp² ⇌ sp rehybridization were responsible for the slow solvolyses of vinyl derivatives, the discussion of Figure 2 implies that the reverse reaction should also be slow, and vinyl cations should not be extraordinarily reactive intermediates but rather sluggish electrophiles. Although rate constants for the reactions of vinyl cations generated by laser-flash photolysis with a variety of nucleophiles have previously been reported,^{33,34} a systematic comparison of the electrophilic reactivities of vinyl cations and tricoordinated carbenium ions has not yet been performed. We now report on a systematic analysis of the reactivities of vinyl cations and show that exceptionally high intrinsic barriers account for their extraordinarily slow formation in S_N1 reactions as well as for their slow reactions with nucleophiles.

RESULTS

Vinyl cations **2** and **3** (Chart 1), which can be generated by laser flash photolysis from **4-Br** and **5-Br**, were selected as representative vinyl cations to study the rates of the reactions with nucleophiles **6–22** (Table 1) in MeCN (**13** and **14** in 2,2,2-trifluoroethanol, TFE) and with the solvent mixtures **23–41** listed in Table 2.

PRODUCT CHARACTERIZATION

Vinyl cations **2** and **3** can be transiently generated in solvents of high ionizing power by heterolysis of precursor vinyl halides or

Chart 1. Structures of Vinyl Cations 2 and 3 and Vinyl Derivatives 4-X and 5-X

pseudohalides **4-X** and **5-X**.^{25,27,39,40a,41} We have found that heterolyses of **4-OMs** and **5-Br** occur at convenient rates at 40 °C in 2,2,2-trifluoroethanol (TFE), a solvent of low nucleophilicity ($N_1 = 1.11$).³⁵ When the vinyl cations are generated in aqueous TFE, the ketones **42** and **43** are formed quantitatively, as shown in [Scheme 2a](#).

To verify that the vinyl cations generated in TFE solution can also be intercepted by other nucleophiles, **4-OMs** and **5-Br** were dissolved in TFE containing $\geq 1 \text{ mol L}^{-1}$ of **10** or **20** as representative nucleophiles. Following our previously published method for carrying out Friedel–Crafts-type chemistry in neutral aqueous or alcoholic solutions,⁴² high nucleophile concentrations were employed to avoid trapping by trifluoroethanol or traces of water. In this way, the reactions of solvolytically generated **2** and **3** with pyrrole **10** ($N = 8.01$ in MeCN) resulted in high conversion to 3-vinylpyrroles **44** and **45**, respectively ([Scheme 2b](#)), without formation of hydrolysis products.⁴³ The reaction of **2** with $[\text{tBu}_4\text{N}]\text{OAc}$ (**20**; $N = 16.9$ in MeCN) gave vinyl acetate **46** ([Scheme 2c](#)) as the major product, with the formation of a small amount (5%) of hydrolysis product **42**.

Table 2. Nucleophile-Specific Reactivity Parameters N_1 and s_N for Solvents and Solvent Mixtures (v/v) 23–41³⁸

nucleophile		N_1	s_N
TFE ^a	23	1.11 ^a	0.96 ^a
TFE/H ₂ O (90:10)	24	2.93	0.88
TFE/H ₂ O (60:40)	25	3.42	0.90
MeCN/H ₂ O (90:10)	26	4.56	0.94
MeCN/H ₂ O (80:20)	27	5.02	0.89
MeCN/H ₂ O (67:33)	28	5.02	0.90
MeCN/H ₂ O (50:50)	29	5.05	0.89
MeCN/EtOH (90:10)	30	5.19	0.96
MeCN/EtOH (80:20)	31	5.77	0.92
MeCN/EtOH (67:33)	32	6.06	0.90
MeCN/EtOH (50:50)	33	6.37	0.90
MeCN/EtOH (33:67)	34	6.74	0.89
MeCN/EtOH (20:80)	35	6.94	0.90
MeCN/EtOH (10:90)	36	7.10	0.90
EtOH/H ₂ O (40:60)	37	5.81	0.90
EtOH/H ₂ O (50:50)	38	5.96	0.89
EtOH/H ₂ O (60:40)	39	6.28	0.87
EtOH/H ₂ O (80:20)	40	6.68	0.85
EtOH/H ₂ O (90:10)	41	7.03	0.86

^aTFE = 2,2,2-trifluoroethanol; N_1 and s_N are taken from ref 35.

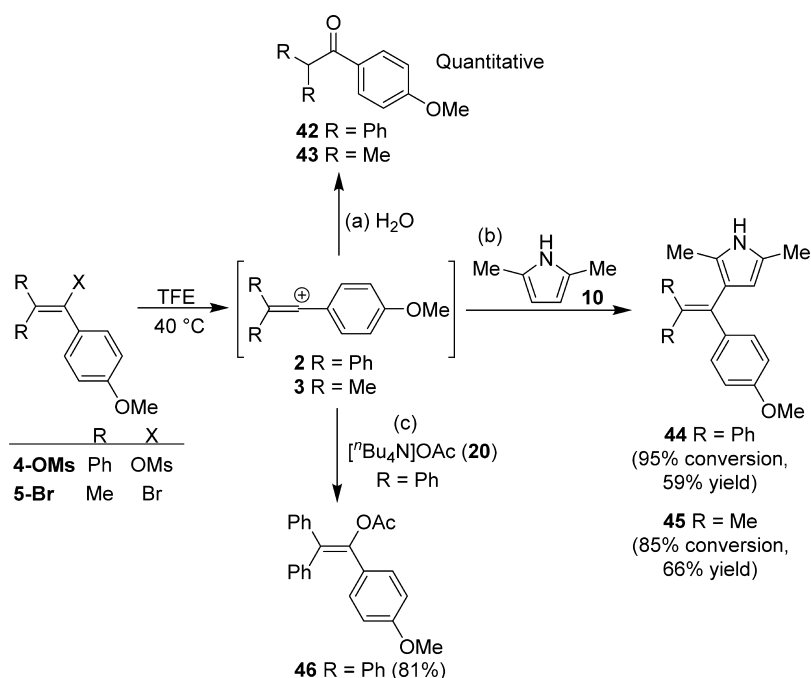
ipso-Substitution (at C-4 of the anisyl group), which has been observed in reactions of photochemically generated vinyl cations **2** with cyanide or alkoxide,^{44,45} but not with alcohols,^{45e,f} did not occur under the conditions described in [Scheme 2](#). We therefore conclude that all nucleophiles were added to the cationic sp-center of **2** and **3** in our kinetic experiments, in line with results from earlier studies carried out under similar conditions.^{33,34,39,40,45e,f,46–49}

Table 1. Structures and Values of the Nucleophile-Specific Parameters N and s_N (in MeCN unless Otherwise Indicated) for Nucleophiles 6–22^{36,37}

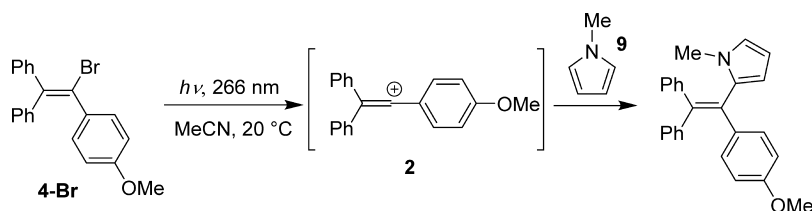
Nucleophile	#	N	s_N	Ref	Nucleophile	#	N	s_N	Ref
	6	3.76	0.91	35		15	12.35	0.72	37
	7	4.41	0.96	24		16	13.77	0.70	37
	8	5.21	1.00	24		17	15.10	0.73	37
	9	5.85	1.03	36		18	15.65	0.74	37
	10	8.01	0.96	36		19	17.35	0.68	37
	11	9.11	0.88	24	$[\text{tBu}_4\text{N}]^{\oplus}\text{OAc}^{\ominus}$	20	16.90	0.75	21
	12	10.13	0.75	37	$[\text{tBu}_4\text{N}]^{\oplus}\text{OMs}^{\ominus}$	21	-	-	-
$[\text{tBu}_4\text{N}]^{\oplus}\text{Cl}^{\ominus}$	13	10.3 ^a	0.60	19	$[\text{tBu}_4\text{N}]^{\oplus}\text{I}^{\ominus}$	22	-	-	-
$[\text{tBu}_4\text{N}]^{\oplus}\text{Br}^{\ominus}$	14	11.7 ^a	0.60	19					

^aSolvent = 2,2,2-trifluoroethanol (TFE).

Scheme 2. Reactions of Vinyl Cations 2 and 3, Generated by Ionization of 4-OMs and 5-Br, Respectively, in TFE in the Presence of Different Nucleophiles



Scheme 3. Generation of Vinyl Cation 2 by Laser Flash Photolysis of 4-Br in MeCN, and Subsequent Reaction with Pyrrole 9



KINETIC INVESTIGATIONS

Vinyl cations **2** and **3** were generated in MeCN, 2,2,2-trifluoroethanol, or solvent mixtures (Tables 1 and 2) by irradiation of the precursor vinyl bromides **4-Br** and **5-Br** with a 7 ns laser pulse of $\lambda = 266$ nm. A single signal is observed in the UV–vis spectrum of each transient cation.⁵⁰ In the presence of a large excess of the nucleophiles **6–22** (pseudo first-order conditions), the absorbance of the vinyl cation was generally observed to undergo monoexponential decay, as shown for the reaction of **2** with **9** (Scheme 3) in Figure 3a.⁵¹ Least-squares fitting of the single-exponential function $A_t = A_0 e^{-k_{\text{obs}}t} + C$ (A_0 and A_t are the absorbances at time 0 and time t , respectively, and C is a constant) to the absorbance decay curve for the reaction of **2** or **3** with a nucleophile yielded k_{obs} (s^{-1}) for the particular concentration of nucleophile.

Plots of the pseudo first-order rate constants k_{obs} versus concentrations of the nucleophile were linear (see Figure 3b) and can be expressed by eq 3:

$$k_{\text{obs}} = k[\text{Nu}] + k_{\text{solv}} \quad (3)$$

where $[\text{Nu}]$ is the molar concentration of the nucleophile, k (the slope of a plot of k_{obs} vs $[\text{Nu}]$) is the second-order rate constant for the reaction of vinyl cation with nucleophile (values in Table 3), and the intercept is the first-order rate constant for the reaction of the vinyl cation with solvent (k_{solv}). Nine of the 14 correlations in acetonitrile showed intercepts in

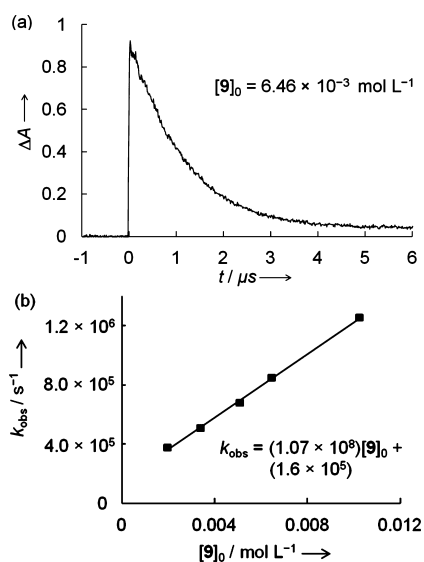
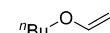

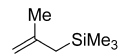
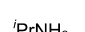
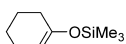
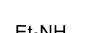
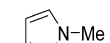
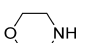
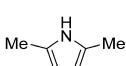
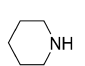
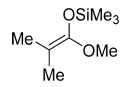

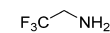


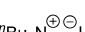
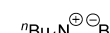


Figure 3. (a) Decay curve ($\lambda = 350$ nm) for the reaction of vinyl cation **2** with pyrrole **9**. (b) The second-order rate constant k was obtained from the slope of the plot of k_{obs} versus $[\mathbf{9}]_0$.

the range $(1.4\text{--}1.7) \times 10^5 \text{ s}^{-1}$, which we ascribe to the reaction of **2** with acetonitrile. The only strong deviation from this value ($6 \times 10^6 \text{ s}^{-1}$, for the reaction of **2** with the strong nucleophile

Table 3. Second-Order Rate Constants, k (20 °C), for the Reactions of Vinyl Cation 2 with Nucleophiles 6–22 (Solvent MeCN unless Otherwise Indicated)

Nucleophile	k (L mol ⁻¹ s ⁻¹)	Nucleophile	k (L mol ⁻¹ s ⁻¹)
 6	1.64×10^5	 15	1.23×10^7
 7	3.10×10^5	 16	4.64×10^7
 8	1.30×10^6	 17	1.28×10^8
 9	1.07×10^8	 18	2.18×10^8
 10	3.17×10^8	 19	6.88×10^8
 11	1.50×10^7	 20	4.79×10^9
 12	6.01×10^6	 21	5.99×10^7
 13	8.06×10^5 ^a	 22	ca. 4.4×10^9 ^b
 14	3.67×10^6 ^a		

^aSolvent = 2,2,2-trifluoroethanol (TFE). ^bApproximate rate constant derived from an experiment with a single concentration of [Bu₄N]I. See details in Supporting Information, p S25.

20) is likely to be a consequence of the problematic extrapolation of the very large rate constants to the concentration [20] = 0. Whereas the intercept for the correlation of k_{obs} versus [Bu₄N]Cl (13) in trifluoroethanol agrees exactly with the previously reported rate constant for the reaction of 2 with trifluoroethanol (nucleophile 23), for unknown reasons the corresponding plot of k_{obs} versus [Bu₄N]Br (14) gives an intercept that is 2 times larger.

Monoexponential decays of the absorbances of the vinyl cations 2 and 3 were also observed when they were generated in trifluoroethanol (23) and in the solvent mixtures 24–41 (see Figure 4 for an example), and the first-order rate constants k_{obs}

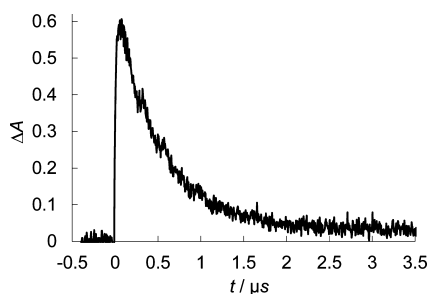


Figure 4. Decay curve ($\lambda = 350$ nm) from the reaction of vinyl cation 2 with 67:33 MeCN/EtOH (32).

were obtained from fitting of $A_t = A_0 e^{-k_{\text{obs}}t} + C$ to the decay curves. However, k_{obs} did not increase linearly with [H₂O] (Figure 5) and remained almost constant when the water content was raised beyond 20% v/v H₂O, in line with previous reports on the consumption of benzhydrylium^{38,52} and tritylium ions⁵² in MeCN/H₂O mixtures. Because a similar situation was also observed for other solvent mixtures, Table 4

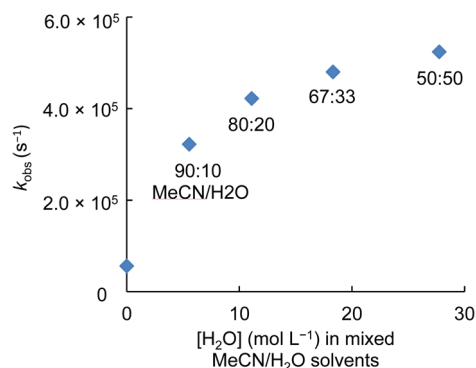


Figure 5. Plot of k_{obs} for the consumption of 2 in MeCN/H₂O solvents versus concentration of H₂O.

lists the first-order rate constants $k = k_{\text{obs}}$ for reactions of 2 with the solvent nucleophiles 23–41.

Second-order rate constants for the reactions of 3 with pyrroles 9 and 10 and first-order rate constants for the reactions of 3 with the solvents 23–27, 30, and 31 were derived in a manner similar to that described above for vinyl cation 2. The rate constants determined in this way are shown in Table 5.

CORRELATIONS AND DISCUSSION

In numerous investigations, we have shown that the second-order rate constants k for the reactions of electrophiles with nucleophiles at 20 °C may be calculated using eq 4:

$$\lg k(20^\circ\text{C}) = s_{\text{N}}(E + N) \quad (4)$$

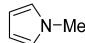
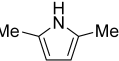
where E characterizes the electrophilicity of the electrophile (treated as being solvent-independent), while N represents the nucleophilicity of the nucleophile, and s_{N} is a nucleophile-

Table 4. First-Order Rate Constants, k (20 °C), for the Reactions of Vinyl Cation 2 with Solvent Nucleophiles 23–41

nucleophile		k (s ⁻¹)
TFE	23	1.4×10^{4a}
TFE/H ₂ O (90:10)	24	2.47×10^4
TFE/H ₂ O (60:40)	25	6.86×10^4
MeCN/H ₂ O (90:10)	26	3.22×10^5
MeCN/H ₂ O (80:20)	27	4.22×10^5
MeCN/H ₂ O (67:33)	28	4.80×10^5
MeCN/H ₂ O (50:50)	29	5.24×10^5
MeCN/EtOH (90:10)	30	6.06×10^5
MeCN/EtOH (80:20)	31	1.05×10^6
MeCN/EtOH (67:33)	32	2.01×10^6
MeCN/EtOH (50:50)	33	3.02×10^6
MeCN/EtOH (33:67)	34	4.13×10^6
MeCN/EtOH (20:80)	35	5.14×10^6
MeCN/EtOH (10:90)	36	6.93×10^6
EtOH/H ₂ O (40:60)	37	1.47×10^6
EtOH/H ₂ O (50:50)	38	1.61×10^6
EtOH/H ₂ O (60:40)	39	1.77×10^6
EtOH/H ₂ O (80:20)	40	2.88×10^6
EtOH/H ₂ O (90:10)	41	4.03×10^6

^aRate constant taken from ref 33.

Table 5. Rate Constants, k (20 °C), for the Reactions of Vinyl Cation 3 with π -Nucleophiles 9 and 10 and with Solvent Nucleophiles 23–27, 30, and 31

Nucleophile		k
 N-Me	9	3.19×10^9 L mol ⁻¹ s ^{-1 a}
 Me	10	1.21×10^9 L mol ⁻¹ s ^{-1 a}
TFE	23	2.3×10^5 s ^{-1 b}
TFE/H ₂ O (90:10)	24	5.85×10^5 s ⁻¹
TFE/H ₂ O (60:40)	25	1.76×10^6 s ⁻¹
MeCN/H ₂ O (90:10)	26	1.30×10^7 s ⁻¹
MeCN/H ₂ O (80:20)	27	1.46×10^7 s ⁻¹
MeCN/EtOH (90:10)	30	1.62×10^7 s ⁻¹
MeCN/EtOH (80:20)	31	2.70×10^7 s ⁻¹

^aSolvent = MeCN. ^bRate constant taken from ref 33. TFE = 2,2,2-trifluoroethanol.

specific susceptibility parameter.^{24,53} Whereas new N and s_N parameters of nucleophiles are derived from linear plots of $\lg k$ versus the known E parameters of the reference electrophiles, new E parameters of electrophiles have been derived from linear correlations between $(\lg k)/s_N$ and N of the reference nucleophiles.

Following this procedure, $(\lg k)/s_N$ was plotted versus N for all investigated nucleophiles with known nucleophilicity parameters (Figure 6). As the published reactivity parameters N and s_N for nucleophiles 6–20 refer to second-order rate constants in acetonitrile, while those for solvents 23–41 (designated N_1) refer to first-order rate constants, it is possible to plot the logarithms of the second-order rate constants for the π -systems 6–11, the amines 12 and 15–19, and the anions 13,

14, and 20, as well as those of the first-order rate constants for the solvents 23–41 side by side in Figure 6. The remarkably good correlation for these diverse nucleophiles over a reactivity range of more than 16 orders of magnitude shows that the nucleophilic reactivities toward vinyl cation 2 (sp²-electrophile) follow the same pattern as those toward benzhydrylium ions. However, eq 4 is not fulfilled because the slope of this correlation is 0.53 and not 1.0, as required by eq 4, showing that 2 is substantially less sensitive to changes in the reactivity of the nucleophile than are benzhydrylium ions (sp²-electrophiles).

A similar plot, shown in Figure 7, was constructed using the first- and second-order rate constants k (listed in Table 5) for the reactions of vinyl cation 3 with a variety of nucleophiles. Again, a strong linear correlation is observed over a wide range of reactivity, and again a slope of much less than 1 is obtained. It is remarkable that even pyrrole 10 fits this correlation although the rate constant of 1.21×10^9 L mol⁻¹ s⁻¹ is already close to the diffusion control limit. Vinyl cation 3 thus shows behavior similar to that of 2. Its higher electrophilic reactivity may be due to reduced steric shielding of the cationic carbon center.

Analogous linear correlations of $\lg k/s_N$ versus N with slopes much smaller than 1 were previously found for S_N2 reactions of alkyl halides,⁵⁴ indicating that variation of the nucleophiles also had a smaller influence on the rate constants of the S_N2 reactions than on those for the reactions with benzhydrylium ions. Although the correlations shown in Figures 6 and 7 might also be mathematically expressed by adding an additional electrophile-specific susceptibility parameter s_E to eq 4,⁵⁴ we refrain from deriving electrophilicity parameters E from the extended correlations. The reason is that E determined in this way would represent an approximate reactivity ranking toward very weak nucleophiles, which react with rate constants close to 1 ($\lg k = 0$), that is, reactions that have little relevance in practice, because commonly used solvents react much faster.

For that reason, let us directly compare rate constants for the reactions of nucleophiles with vinyl cations 2 and 3 and with benzhydrylium ions 47–49 (Chart 2).

In Figure 8, the $\lg k$ values for the reactions of 2 (values of k taken from Tables 3 and 4) are plotted against the corresponding $\lg k$ values for the reactions of benzhydrylium ion 47 ($k(47)$ from Table S1 on pp 43–44 of the Supporting Information).⁵⁵ The plot shows a fair correlation between the two data sets and (similar to Figure 6) that the rate constants for the reactions with the vinyl cation 2 are less affected by variation of the nucleophiles than the corresponding rate constants for 47 (slope = 0.48). If we neglect the two pyrroles (9 and 10), which deviate significantly from the correlation, one can see that the vinyl cation 2 reacts faster than the dimethoxybenzhydrylium ion 47 with weak nucleophiles ($k < 5 \times 10^6$ s⁻¹ or L mol⁻¹ s⁻¹), while stronger nucleophiles react faster with benzhydrylium ion 47. Overall, however, the vinyl cation 2 and the dimethoxybenzhydrylium ion 47 have comparable electrophilic reactivities.

An analogous comparison can be made between vinyl cation 3 and benzhydrylium ion 48. A plot of $\lg k$ for the reactions of 3 with various nucleophiles versus $\lg k$ for the corresponding reactions of 48 ($k(48)$ from Table S2 on p S44 of the Supporting Information) shows a good linear correlation (Figure 9),⁵⁶ with a slope significantly less than 1 (slope = 0.56). Vinyl cation 3 thus has an electrophilicity comparable to that of 48.

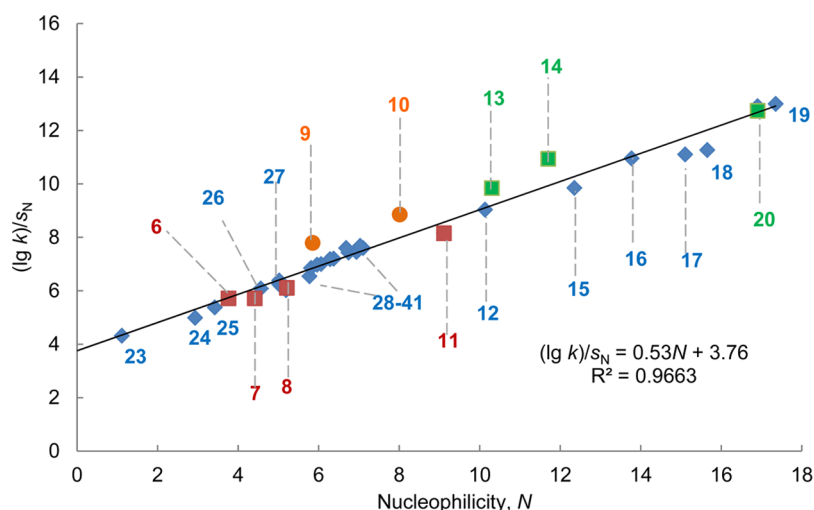


Figure 6. Plot of $\lg k/s_N$ versus N for the reactions of vinyl cation 2 with nucleophiles 6–20 and 23–41.

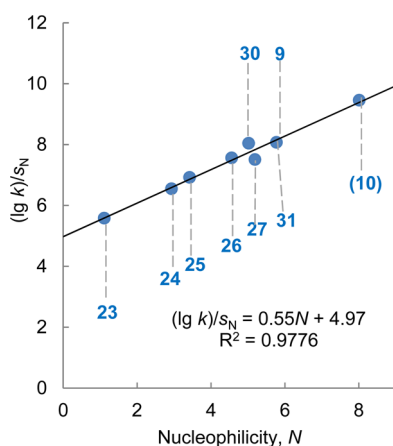
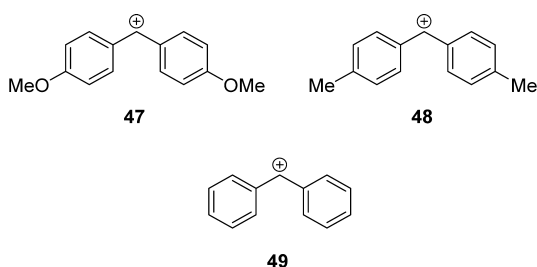


Figure 7. Plot of $\lg k/s_N$ versus N for vinyl cation 3, from its reactions with various nucleophiles.

Chart 2. Benzhydrylium Ions 47–49



The observation that vinyl cations 2 and 3 show reactivities toward nucleophiles that are similar to the corresponding reactivities of the donor-stabilized benzhydrylium ions 47 and 48 appears surprising at first glance, as the latter species are formed much faster in S_N1 reactions than the corresponding vinyl derivatives. In fact, the ionizations of the benzhydryl bromides, which yield the highly stabilized benzhydryl cations 47 and 48, are so fast in aqueous ethanol that it is not possible at present to measure the corresponding solvolysis rates.

Therefore, we compare here the solvolyses of the vinyl bromides 4-Br and 5-Br with that of Ph_2CHBr (for which experimental data are available). Scheme 4 shows that the benzhydryl bromide solvolyzes 10^5 – 10^6 times faster in 80%

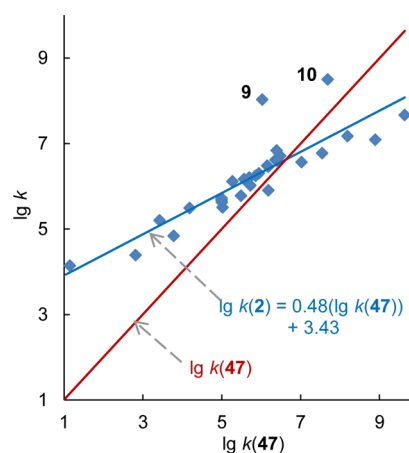


Figure 8. Correlation of $\lg k$ for the reactions of vinyl cation 2 with various nucleophiles (6–16, 23–41) with $\lg k$ for the analogous reactions of the 4,4'-dimethoxybenzhydrylium ion 47 (from Table S1). The red line is a plot of $\lg k(47)$ against itself to highlight the crossing range where nucleophiles react with equal rates with 2 and 47.

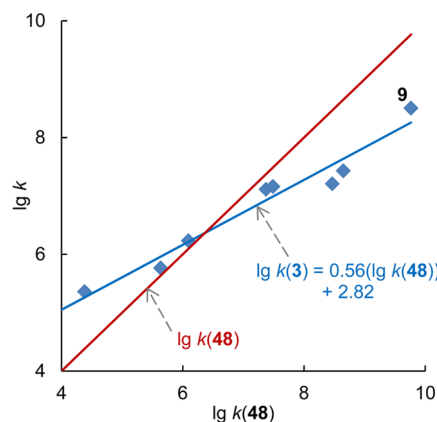
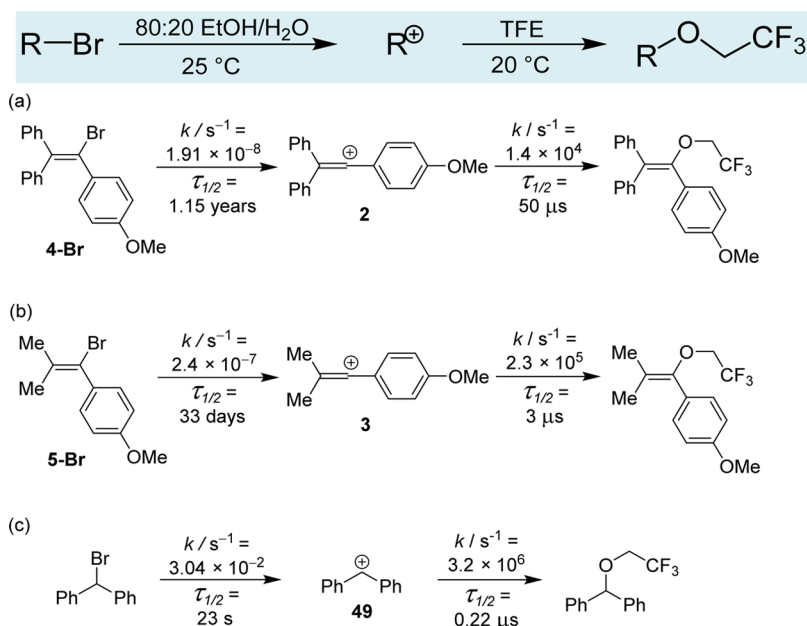


Figure 9. Correlation of $\lg k$ for the reactions of vinyl cation 3 with various nucleophiles (9, 23–27, 30, 31) with $\lg k$ for the analogous reactions of the 4,4'-dimethylbenzhydrylium ion 48 (from Table S2). The red line is a plot of $\lg k(48)$ against itself to highlight the crossing range where nucleophiles react with equal rates with 3 and 48.

Scheme 4. Solvolysis Reactions of (a) 4-Br, (b) 5-Br, and (c) Ph₂CHBr in 80:20 EtOH/H₂O at 25 °C, and Reactions of Cations 2, 3, and 49 with TFE at 20 °C

(a) For the first step of reaction (a), a value of $k = 1.92 \times 10^{-4} \text{ s}^{-1}$ was measured at 120 °C;^{39d} reported activation parameters allow extrapolation to value at 25 °C given in the scheme. The rate constant for the second step is taken from ref 33. (b) For the first step of reaction (b), a value of $k = 8.78 \times 10^{-4} \text{ s}^{-1}$ was measured at 120 °C;^{40c} reported activation parameters allow extrapolation to the value at 25 °C given in the scheme. The rate constant for the second step is taken from ref 33. (c) The rate constant for the first step of (c) is from ref 57. The rate constant for the second step is from ref 58.

aqueous ethanol at 25 °C than the vinyl bromides 4-Br and 5-Br. Despite its much faster rate of formation, the parent benzhydrylium ion reacts 1–2 orders of magnitude faster with trifluoroethanol at 20 °C than 2 or 3 (compare the second reactions in each of Scheme 4a–c). Similar rate ratios have been found for activation-controlled reactions of these electrophiles with numerous other nucleophiles (i.e., reactions that do not proceed with diffusion-controlled rates).

Laser flash experiments have shown that the reactions of the parent benzhydrylium ion 49 with Br[−] are diffusion-controlled in all alcoholic solvents investigated.¹⁹ As there is no barrier for the ion combination, the principle of microscopic reversibility implies that the transition state for the heterolytic cleavage of Ph₂CHBr corresponds to the ion-pair, as illustrated in Figure 10.

In contrast, the reaction of Br[−] with vinyl cation 2 is activation controlled, proceeding with a rate constant of $3.7 \times 10^6 \text{ L mol}^{-1} \text{ s}^{-1}$ in TFE (Table 3). For the same reaction in 80% aqueous ethanol, one can calculate $k = 7.4 \times 10^6 \text{ L mol}^{-1} \text{ s}^{-1}$ from $N = 14.5$, $s_N = 0.6$ (for Br[−] in 80% aqueous ethanol)¹⁹ using the correlation equation given in Figure 6. As this reaction is not diffusion-controlled, transition state theory can be applied to calculate an activation energy of $\Delta G^\ddagger = 8.1 \text{ kcal mol}^{-1}$ for the ion combination in 80% aqueous ethanol (Figure 10, right-hand side). The kinetic data imply that the heterolyses of Ph₂CHBr and 4-Br have almost identical ΔG° values, as shown in Figure 10.

Figure 10 clearly illustrates that the major reason for the different solvolysis rates of Ph₂CHBr and 4-Br is the difference in the intrinsic barriers (because the Gibbs energies of reaction ΔG° are very similar). Hence, the transition state of the first step of the S_N1 reaction of 4-Br cannot be carbocation-like; that is, it does not correspond to the ion pair of Br[−] with vinyl

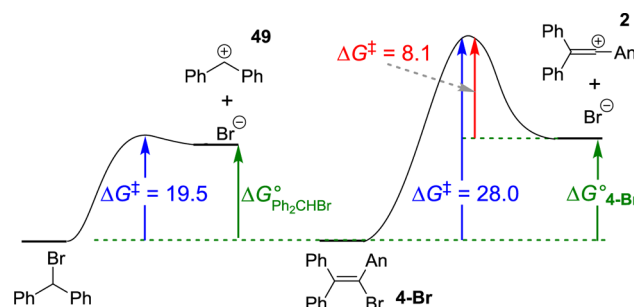


Figure 10. Schematic Gibbs energy profiles (kcal mol^{−1}) for the ionization of benzhydryl bromide and vinyl bromide 4-Br in 80% aqueous ethanol at 25 °C. ΔG^\ddagger values were calculated using the Eyring equation (for the solvolysis reactions, rate constants from Scheme 4a and c were used; see the main text for details of the calculation for addition of Br[−] to 2).

cation 2. We demonstrate explicitly below using quantum chemical calculations that $\Delta\Delta G^\circ = \Delta G^\circ_{\text{Ph}_2\text{CHBr}} - \Delta G^\circ_{4\text{-Br}}$ is indeed negligible (vide infra), as derived from kinetic data for the construction of Figure 10.

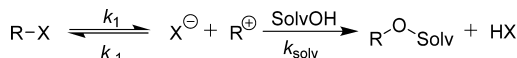
COMMON ION RATE DEPRESSION

Although S_N1 reactions are usually accelerated when the polarity of the solvent is increased by salt additives,^{1c,d,h,59} in certain cases, the opposite effect is observed. Common ion rate depression is a phenomenon whereby the rate of a solvolysis reaction k_{obs} is slowed by addition of a salt containing the anion of the leaving group (X[−]).^{1h,19,27,60} It is observed when the recombination of the carbocation R⁺ with X[−] is faster than addition of the solvent to R⁺ (with first-order rate constant

k_{solv}), that is, when $k_{-1}[X^-] \geq k_{\text{solv}}$ (see Scheme 5, and eq 5, in which the full expression for k_{obs} is given, and $\alpha = k_{-1}/k_{\text{solv}}$).

$$k_{\text{obs}} = \frac{k_1 k_{\text{solv}}}{k_{\text{solv}} + k_{-1}[X^-]} = \frac{k_1}{1 + \alpha[X^-]} \quad (5)$$

Scheme 5. Reversible Heterolysis of RX To Give R⁺, Which May React with Solvent (Completing the Solvolysis) or Revert to RX by Reaction with X⁻



As highly reactive carbocations are immediately trapped by the solvent, which is present in high concentration, common ion return is only observed when highly stabilized carbocations are generated in solvents of low nucleophilicity. Since vinyl cations had been considered to be highly reactive because of their slow formation in the S_N1 processes, the observation of common ion rate depression in S_N1 processes was highly surprising, and the numerous attempts to rationalize this phenomenon have been summarized.^{60b} With the knowledge that vinyl cations 2 and 3 have relatively low electrophilic reactivities, similar to those of the highly stabilized benzhydrylium ions 47 and 48 (see Figures 8 and 9), two systems for which common ion depression has generally been observed,¹⁹ it is no longer surprising that this effect was also found for the solvolyses of 4-X and 5-X (X = Cl, Br).^{60b}

In previous work, we have demonstrated that the occurrence of common ion rate depression can be derived from the directly measured rate constants of the reactions of the independently generated carbocations with the anionic leaving groups (i.e., X⁻) and the solvent.¹⁹ From the rate constants in Tables 3 and 4 for the reactions of 2 with Cl⁻ in TFE (8.06 × 10⁵ L mol⁻¹ s⁻¹), Br⁻ in TFE (3.67 × 10⁶ L mol⁻¹ s⁻¹), and TFE (1.40 × 10⁴ s⁻¹), respectively, one can calculate α values of 58 and 262, respectively, in good agreement with common ion rate depressions observed for similar systems under comparable conditions.⁶¹

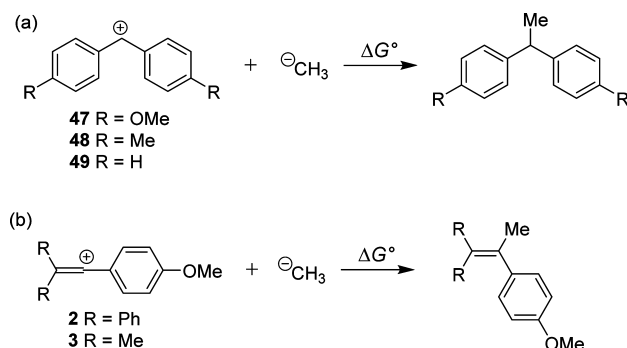
COMPUTATIONAL ANALYSIS

Directly measured rate constants as well as the observation of common ion rate depression thus indicate that vinyl cations are sluggish electrophiles, despite their very slow formation in S_N1 reactions. By combining the experimentally determined rate constants for the solvolysis reactions and ion recombinations (see Figure 10 and associated discussion above), we had derived that ΔG° for the heterolytic cleavage of the C–Br bond in Ph₂CHBr is almost the same as that for heterolysis of 4-Br. This conclusion is in line with quantum chemical calculations, as we show below.

Recently, we have calculated⁶² gas-phase methyl anion affinities of benzhydrylium ions as a measure for their relative Lewis acidities (Scheme 6, table entries 1–3).¹² Comparison with entries 4 and 5 shows that the methyl anion affinities of vinyl cations 2 and 3 are closely similar to that of the unsubstituted benzhydrylium ion (49), as was independently derived from the rate constants for forward and backward reactions in Figure 10.⁶³ Kinetic data and quantum chemically calculated Lewis acidities thus agree on the conclusion that the differences in intrinsic barriers account for the fact that vinyl cations 2 and 3, despite their much higher Lewis acidities, are not more electrophilic than the highly stabilized benzhydrylium ions 47 and 48, respectively (Figures 8 and 9 and associated discussion).

The calculations shown in Table 6 confirm that in the gas phase, Ph₂CH⁺ and 2 also have almost equal affinities toward Br⁻ ($\Delta\Delta G^\circ = 0.9$ kcal mol⁻¹, entries 1, 2) as well as toward Br⁻ solvated by one

Scheme 6. Calculated Gibbs Energies of Reactions of Methyl Anion with Benzhydrylium Ions 47–49 and of Vinyl Cations 2 and 3 (Methyl Anion Affinities) in the Gas Phase



Entry		R	ΔG° (kcal mol ⁻¹)
1	47	OMe	-178.9 ^b
2	48	Me	-188.6 ^b
3	49	H	-197.7 ^b
4	2	Ph	-198.2 ^c
5	3	Me	-200.2 ^c

(a) Computational method and basis set employed for all values of ΔG° : B3LYP/6-311++G(3df,pd)//B3LYP/6-31G(d,p).^{62,64} (b) Calculated value reported in ref 12. (c) This work.^{62–64}

Table 6. Calculated Gibbs Energies of the Reactions of Br⁻ (and Br⁻ Solvated by 1 Water Molecule) with the Parent Benzhydrylium Ion (49) and Vinyl Cation 2 in the Gas Phase^a and in Aqueous Solution^b

$$\text{R}^\oplus + \text{X}^\ominus \xrightarrow{\Delta G^\circ \text{ (kcal mol}^{-1}\text{)}} \text{R-X}$$

entry	R ⁺	X ⁻	gas phase/solvent model	ΔG° (kcal mol ⁻¹)
1	Ph ₂ CH ⁺	Br [⊖]	gas	-113.9
2	2	Br [⊖]	gas	-114.8
3	Ph ₂ CH ⁺	Br [⊖] (H ₂ O) ₁	gas	-102.1
4	2	Br [⊖] (H ₂ O) ₁	gas	-103.2
5	Ph ₂ CH ⁺	Br [⊖]	water	-9.5
6	2	Br [⊖]	water	-15.3
7	Ph ₂ CH ⁺	Br [⊖] (H ₂ O) ₁	water	-5.8
8	2	Br [⊖] (H ₂ O) ₁	water	-11.6

^aComputational method and basis set employed for all values of ΔG° : TPSSTPSS/def2TZVP+GD3.^{66,67} ^bPCM; method TPSSTPSS/def2TZVP+GD3. See Table S7 (p S83 of Supporting Information) for further quantities determined from these calculations.

molecule of water ($\Delta\Delta G^\circ = 1.1$ kcal mol⁻¹, entries 3, 4), in agreement with our observations based on the kinetic data (Figure 10). As expected, the ion combinations are calculated to be much less exergonic in solution (entries 5–8), but the very small calculated values of ΔG° in aqueous solution indicate that the PCM model significantly overestimates the ion solvation energies.⁶⁵

When trying to localize the transition states for the heterolytic cleavage reactions of 4-Br and Ph₂CHBr in aqueous solution (i.e., the reactions in Figure 10) by the DFT method TPSSTPSS/def2TZVP+GD3 using the PCM continuum solvent model,⁶⁸ we observed a continuous increase of the potential energy (E_{tot}) as the C–Br bond length was elongated, and the ion pair was reached without passing through a maximum in E_{tot} (Figure 11). The same result was found when one molecule of water was explicitly considered (see Figure S4 in the Supporting Information, p S84). In both cases, the gradient was

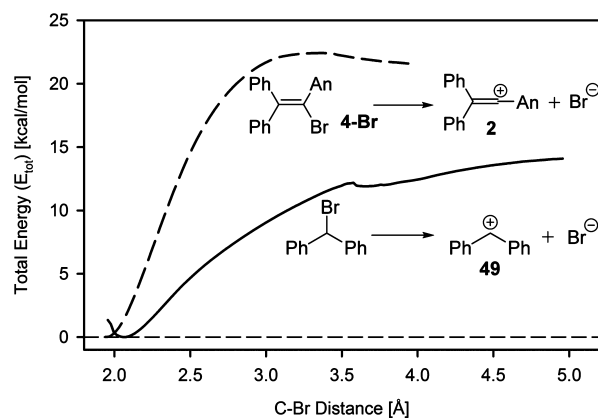


Figure 11. Intrinsic reaction coordinate calculations for the cleavage of the C–Br bond in **4-Br** and Ph_2CHBr (total energies E_{tot} ; TPSTSPSS/def2TZVP+GD3; PCM (solvent = water)).

much larger for the vinyl bromide due to the higher force constant of the $\text{C}(\text{sp}^2)\text{--Br}$ bond.

The fact that the maximum of total energy in the **4-Br** graph of Figure 11 is slightly lower than ΔE_{tot} calculated for the reaction of **2** with Br^- in water ($-24.9 \text{ kcal mol}^{-1}$, see Table S7 in the Supporting Information on p S83) may be due to shortcomings of the PCM-model (used for the calculations on the heterolysis reactions as well as for those on the separated species) and the fact that for longer C–Br distances the closed-shell restriction does not apply.

A computational assessment of the transition state for the vinyl bromide heterolysis (for which the activation barrier was unequivocally deduced from kinetic data; see Figure 10 and associated discussion) might be possible by explicit consideration of more solvent molecules. However, general problems of this type of treatment have recently been pointed out by Plata and Singleton,⁶⁹ and, in any case, this approach is beyond the scope of this investigation.

As mentioned in the Introduction, the intrinsic barrier in the Marcus equation (ΔG_0^\ddagger) corresponds to the Gibbs activation energy of an identity reaction. Because there are no identity reactions for the ion combinations in eq 1, we analyzed the intrinsic barriers for the identity hydride transfers illustrated in Scheme 7 as models for the transition states of $\text{sp}^3 \rightleftharpoons \text{sp}^2$ and $\text{sp}^2 \rightleftharpoons \text{sp}$ rehybridizations (Table 7).⁷⁰

Table 7 allows comparison of quantum chemically calculated and experimental gas-phase hydride affinities for several tri- and dicoordinated carbenium ions.⁷¹ While the absolute hydride affinities calculated with different basis sets differ considerably (see Supporting Information, pp S69–70), there is good agreement between relative hydride affinities obtained with different computational methods and experimental data.

Table 7 shows, for example, that successive replacement of the methyl groups in the isopropyl cation by phenyl (i.e., giving first phenethyl cation and then benzhydryl cation) reduces the hydride affinities by 25 and then 15 kcal mol^{-1} in calculated ΔH_{HA} and ΔG_{HA}

(entries 1, 3, 6) and in experimentally determined ΔH_{HA} . The hydride affinities of the vinyl cations (entries 2 and 4) are 13 kcal mol^{-1} larger than those of the corresponding saturated analogues (entries 1 and 3).

Hydride transfer to tri- or dicoordinated carbenium ions from their parent alkanes or alkenes occurs through hydrido-bridged species (Scheme 7). The enthalpies and Gibbs energies (ΔH_{bridge} and ΔG_{bridge} , respectively) of formation of these entities from the isolated reactants, that is, the intrinsic barriers for the hydride transfers, are shown in the right-hand columns of Table 7. Whereas the hydrido-bridged species from isopropyl cation/propane (entry 1) and benzyl cation/toluene (entry 5) are minima on the potential energy surface (gas phase), all other hydrido-bridged species correspond to transition states (Table 7, and Tables S4–S6 in the Supporting Information, pp S71–S75). All minima and all transition states have a negative ΔH_{bridge} with respect to the isolated reactants. As expected, the tendency to undergo hydrido-bridging decreases with decreasing hydride ion affinity; that is, for tricoordinated carbenium ions, ΔG_{bridge} increases in the order $1 < 5 \approx 3 < 6$ and in the order entry 2 < entry 4 for dicoordinated carbenium ions.

In the context of our analysis, the comparisons of entries 2 and 1 and of entries 4 and 3 are of particular importance. Although the vinyl cations in entries 2 and 4 have significantly higher hydride affinities as compared to their saturated analogues in entries 1 and 3, respectively, their hydrido-bridging tendencies are much smaller. As the hydrido-bridged complexes represent models for the transition states of $\text{sp}^3 \rightleftharpoons \text{sp}^2$ and $\text{sp}^2 \rightleftharpoons \text{sp}$ rehybridizations (Scheme 7), the 8 kcal/mol lower tendency toward hydrido-bridging of the phenyl-substituted vinyl cation in entry 4 as compared to the saturated analogue in entry 3 reflects the high intrinsic barriers, which are responsible for the low rates of vinyl halide heterolyses (low electrofugalities¹⁵ of vinyl cations) and the low rates of nucleophilic additions to vinyl cations (low electrophilicities¹⁵ of vinyl cations).

CONCLUSION

Discussions of carbocation reactivities are generally based on the assumption that the transition states of $\text{S}_{\text{N}}1$ reactions are carbocation-like (Hammond postulate), and that the slower a carbocation is formed in an $\text{S}_{\text{N}}1$ process, the faster it will react with a nucleophile. Although deviations from this rule have previously been reported, including literature reports on comparatively low absolute rate constants for reactions of vinyl cations with nucleophiles and common ion rate depression in solvolyses of vinyl derivatives (typical for carbocations of relatively low reactivity), the consequences of these observations for the interpretation of vinyl cation chemistry have rarely been considered.

We have now shown that the transition states of vinyl halide solvolyses are often not carbocation-like. Consequently, the influence of intrinsic barriers on this step cannot be neglected. The approximation to consider only the thermodynamic term (i.e., ΔG° of the ionization step) for analyzing the kinetic behavior of carbocations, which works well for the reactions of

Scheme 7. Formation of (a) Tricoordinated and (b) Dicoordinated Hydrido-Bridged Carbenium Ions $[\text{R}^+\text{---H}^+\text{---R}]^+$ from the Isolated Carbenium Ion R^+ and Its Parent Compound, RH (Without Considering Species Showing Aromatic Interactions (π -Stacking))

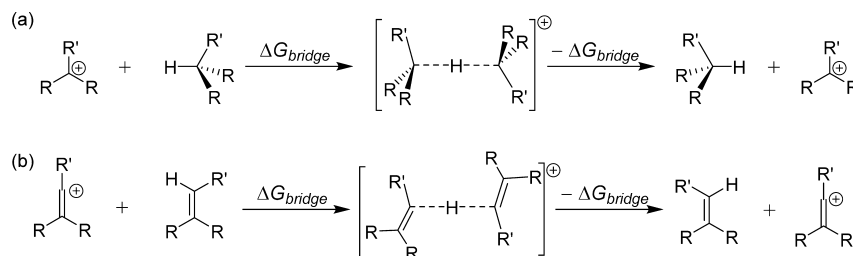
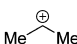
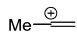
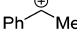
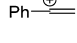
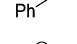
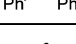


Table 7. Comparison of Calculated and Experimental Gas-Phase Values ΔH_{HA} (298 K) and ΔG_{HA} (298 K) for Additions of H^- to Various Carbenium Ions (Hydride Affinity = $-\Delta H_{\text{HA}}$), and Calculated Intrinsic Barriers ΔH_{bridge} and ΔG_{bridge} for the Hydride Transfer Reactions

$$\text{R-H} \xleftarrow[\Delta H_{\text{HA}}]{\text{H}^-} \text{R}^+ \xrightarrow[\Delta H_{\text{bridge}}]{\text{R-H}} [\text{R}\cdots\text{H}\cdots\text{R}]^{\oplus}$$

Entry	R ⁺	Experimental ΔH_{HA}^a	Calculated Quantities ^b			
			ΔH_{HA}^b	ΔG_{HA}^b	$\Delta H_{\text{bridge}}^b$	$\Delta G_{\text{bridge}}^b$
1		-251.8	-259.3	-251.8	-18.5	-8.1
2		-264.9	-272.4	-264.2	-14.9	-2.9
3		-225.1	-234.5	-228.0	-12.2	+0.3
4		-239.7	-247.5	-240.1	-3.8	+8.2
5		-239.3	-246.8	-240.6	-12.9	-1.9
6		-	-220.9	-212.8	-8.0	+3.3

^aExperimental data (kcal mol⁻¹) listed in ref 30. ^bCalculated values from this work. Method and basis set employed: TPSS/TPSS/def2TZVP+GD3. Units are kcal mol⁻¹.

most weakly stabilized tricoordinated carbenium ions, cannot be applied for vinyl cations. Vinyl cations (i.e., dicoordinated carbenium ions) are weaker electrofuges as well as weaker electrophiles than tricoordinated carbenium ions of similar Lewis acidity because of the high intrinsic barriers for $\text{sp}^2 \rightleftharpoons \text{sp}$ rehybridizations.

■ ASSOCIATED CONTENT

Supporting Information

The Supporting Information is available free of charge on the ACS Publications website at DOI: 10.1021/jacs.6b10889.

Experimental procedures and characterization of representative products; details of kinetic experiments with vinyl cations 2 and 3; literature rate constants used for the construction of Figures 8 and 9; copies of NMR spectra; and details of quantum chemical calculations (PDF)

■ AUTHOR INFORMATION

Corresponding Author

*herbert.mayr@cup.uni-muenchen.de

ORCID

Herbert Mayr: 0000-0003-0768-5199

Notes

The authors declare no competing financial interest.

■ ACKNOWLEDGMENTS

Dedicated to Professor Zvi Rappoport. We thank the Deutsche Forschungsgemeinschaft (SFB 749, Project B1) for financial support, the Humboldt foundation for the provision to P.A.B. of a Humboldt Research Fellowship for Postdoctoral Researchers, Giulio Volpin, Dr. David Stephenson, and Claudia Dubler for assistance with NMR spectroscopy, and Dr. A. R. Ofial for helpful comments.

■ REFERENCES

- General reviews: (a) *Carbonium Ions*, Vols. 1–5; Olah, G. A., Schleyer, P. v. R., Eds.; Interscience: New York, 1968–1976. (b) Olah, G. A. *Angew. Chem.* **1973**, *85*, 183–225; *Angew. Chem., Int. Ed. Engl.* **1973**, *12*, 173–212. (c) Streitwieser, A., Jr. *Solvolytic Displacement Reactions*; McGraw-Hill: New York, 1962. (d) Ingold, C. K. *Structure and Mechanism in Organic Chemistry*, 2nd ed.; Cornell University Press: Ithaca, NY, 1969. (e) Vogel, P. *Carbocation Chemistry*; Elsevier: Amsterdam, 1985. (f) *Advances in Carbocation Chemistry*, Vol. 1; Creary, X., Ed.; JAI Press: Greenwich, CT, 1989. (g) *Advances in Carbocation Chemistry*, Vol. 2; Coxon, J. M., Ed.; JAI Press: Greenwich, CT, 1995. (h) Raber, D. J.; Harris, J. M.; Schleyer, P. v. R. In *Ions and Ion Pairs in Organic Reactions*; Swarc, M., Ed., Wiley and Sons: New York, 1974; Vol. 2, pp 247–374.
- Electrophilicities of carbocations: (a) Ritchie, C. D. *Can. J. Chem.* **1986**, *64*, 2239–2250. and references therein. (b) Mayr, H. *Seminars in Organic Synthesis*; 40th “A. Corbella” International Summer School, Gargnano, Società Chimica Italiana, 2015; pp 82 – 107. (c) Mayr, H.; Ofial, A. R. In *Carbocations*; Olah, G. A., Prakash, G. K. S., Eds.; Wiley: New York, 2004; Chapter 13.
- pK_{R^+} values ($\text{X}^- = \text{HO}^-$): (a) Deno, N. C.; Jaruzelski, J. J.; Schriesheim, A. *J. Am. Chem. Soc.* **1955**, *77*, 3044–3051. (b) Deno, N. C.; Schriesheim, A. *J. Am. Chem. Soc.* **1955**, *77*, 3051–3054. (c) Arnett, E. M.; Bushick, R. D. *J. Am. Chem. Soc.* **1964**, *86*, 1564–1571. (d) Ritchie, C. D.; Fleischhauer, H. *J. Am. Chem. Soc.* **1972**, *94*, 3481–3483. (e) Kitagawa, T.; Takeuchi, K. *J. Phys. Org. Chem.* **1998**, *11*, 157–170. and references therein. (f) Deno, N. C.; Berkheimer, H. E.; Evans, W. L.; Peterson, H. J. *J. Am. Chem. Soc.* **1959**, *81*, 2344–2347. (g) Gandler, J. *J. Am. Chem. Soc.* **1985**, *107*, 8218–8223. (h) Amyes, T. L.; Richmond, J. P.; Novale, M. *J. Am. Chem. Soc.* **1992**, *114*, 8032–8041. (i) Ostovic, D.; Lee, I. S. H.; Roberts, R. M. G.; Kreevoy, M. M. *J. Org. Chem.* **1985**, *50*, 4206–4211. (j) Okamoto, K.; Takeuchi, K.; Komatsu, K.; Kubota, Y.; Ohara, R.; Arima, M.; Takahashi, K.; Waki, Y.; Shirai, S. *Tetrahedron* **1983**, *39*, 4011–4024. (k) See also ref 2a.
- Gas-phase hydride affinities of carbenium ions ($\text{X}^- = \text{H}^-$): (a) Wolf, J. F.; Staley, R. H.; Koppel, I.; Taagepera, M.; McIver, R. T.; Beauchamp, J. L.; Taft, R. W. *J. Am. Chem. Soc.* **1977**, *99*, 5417–5429. (b) Lossing, F. P.; Holmes, J. L. *J. Am. Chem. Soc.* **1984**, *106*, 6917–6920. (c) Schultz, J. C.; Houle, F. A.; Beauchamp, J. I. *J. Am. Chem. Soc.* **1984**, *106*, 3917–3927. (d) Karaman, R.; Huang, J.-T. L.; Fry, J. L. *J. Org. Chem.* **1991**, *56*, 188–195. (e) Zhu, X.-Q.; Wang, C.-H. *J. Phys.*

Chem. A **2010**, *114*, 13244–13256. (f) Kim, C. K.; Lee, K. A.; Bae, S. Y.; Han, I. S.; Kim, C. K. *Bull. Korean Chem. Soc.* **2004**, *25*, 311–313.

(5) Solution hydride affinities of carbenium ions ($X^+ = H^+$): (a) Cheng, J.-P.; Handoo, K. L.; Parker, V. D. *J. Am. Chem. Soc.* **1993**, *115*, 2655–2660. (b) Arnett, E. M.; Flowers, R. A.; Ludwig, R. T.; Meekhof, A. E.; Walek, S. A. *J. Phys. Org. Chem.* **1997**, *10*, 499–513. (c) See also ref 3i. (d) Zhu, X.-Q.; Deng, F.-H.; Yang, J.-D.; Li, X.-T.; Chen, Q.; Lei, N.-P.; Meng, F.-K.; Zhao, X.-P.; Han, S.-H.; Hao, E.-J.; Mu, Y.-Y. *Org. Biomol. Chem.* **2013**, *11*, 6071–6089.

(6) Calorimetric determination of enthalpies of ionization of alkyl halides in SbF_5/SO_2Cl_2 superacid (formally the reverse of the reaction in eq 1b; $X^- = \text{halide}$): (a) Arnett, E. M.; Petro, S. C. *J. Am. Chem. Soc.* **1978**, *100*, 2563–2564. (b) Arnett, E. M.; Petro, S. C. *J. Am. Chem. Soc.* **1978**, *100*, 5402–5407. (c) Arnett, E. M.; Petro, S. C. *J. Am. Chem. Soc.* **1978**, *100*, 5408–5416. (d) Arnett, E. M.; Petro, S. C.; Schleyer, P. v. R. *J. Am. Chem. Soc.* **1979**, *101*, 522–526. (e) Arnett, E. M.; Pienta, N. J. *J. Am. Chem. Soc.* **1980**, *102*, 3329–3334. (f) Arnett, E. M.; Hofelich, T. C. *J. Am. Chem. Soc.* **1983**, *105*, 2889–2895. (g) Arnett, E. M.; Hofelich, T. C. *J. Am. Chem. Soc.* **1982**, *104*, 3522–3524.

(7) Equilibrium constants for ionization of benzhydryl chlorides ($X^- = \text{halide}$): Schade, C.; Mayr, H.; Arnett, E. M. *J. Am. Chem. Soc.* **1988**, *110*, 567–571.

(8) Enthalpies and equilibrium constants for reactions of carbocations with carbanions ($X^- = \text{carbanion}$): (a) Troughton, E. B.; Molter, K. E.; Arnett, E. M. *J. Am. Chem. Soc.* **1984**, *105*, 6726–6735. (b) Arnett, E. M.; Chawla, B.; Molter, K.; Amarnath, K.; Healy, M. *J. Am. Chem. Soc.* **1985**, *107*, 5288–5289. (c) Arnett, E. M.; Molter, K. E. *Acc. Chem. Res.* **1985**, *18*, 339–346.

(9) Gibbs energies of reaction for production of carbocations from neutral precursors in the gas phase, determined using ion cyclotron resonance techniques: (a) Aue, D. H.; Bowers, M. T. *Gas Phase Ion Chemistry*; Academic Press: New York, 1979; Vol. 2, Chapter 9. (b) Walder, R.; Franklin, J. L. *Int. J. Mass Spectrom. Ion Phys.* **1980**, *36*, 85–112. (c) Kebarle, P. *Annu. Rev. Phys. Chem.* **1977**, *28*, 445–476. (d) Abboud, J.-L. M.; Alkorta, I.; Davalos, J. Z.; Müller, P.; Quintanilla, E.; Rossier, J.-C. *J. Org. Chem.* **2003**, *68*, 3786–3796.

(10) Destabilized carbocations: Tidwell, T. T. *Angew. Chem.* **1984**, *96*, 16–28; *Angew. Chem., Int. Ed. Engl.* **1984**, *23*, 20–32.

(11) Gas-phase IR spectroscopy: (a) Crestoni, M. E.; Fornarini, S. *Angew. Chem.* **2012**, *124*, 7487–7489; *Angew. Chem., Int. Ed.* **2012**, *51*, 7373–7375. (b) Chiavolino, B.; Crestoni, M. E.; Dopfer, O.; Maitre, P.; Fornarini, S. *Angew. Chem.* **2012**, *124*, 5031–5033; *Angew. Chem., Int. Ed.* **2012**, *51*, 4947–4949.

(12) Mayr, H.; Ammer, J.; Baidya, M.; Maji, B.; Nigst, T. A.; Ofial, A. R.; Singer, T. *J. Am. Chem. Soc.* **2015**, *137*, 2580–2599.

(13) Abboud, J.-L. M.; Alkorta, I.; Dávalos, J. Z.; Müller, P.; Quintanilla, E. *Adv. Phys. Org. Chem.* **2002**, *37*, 57–135.

(14) Hine, J. *Structural Effects on Equilibria in Organic Chemistry*; Krieger Publishing Company: Huntington, NY, 1981; pp 215–256.

(15) Mayr, H.; Ofial, A. R. *Acc. Chem. Res.* **2016**, *49*, 952–965.

(16) Equilibrium constants have been reported for reversible C–C bond heterolysis in DMSO to give hydrocarbon salts ($X^- = \text{carbanion}$) in ref 3e.

(17) Carbocation reduction potentials (E_{red}) have also been used as a measure of their stability: See refs 3e, 3i, 3j, and 5b.

(18) (a) Stewart, R. *The Proton: Applications to Organic Chemistry*; Academic Press: Orlando, 1985; p 125. (b) Kresge, A. J.; Chen, H. J.; Hakka, L. E.; Kouba, J. E. *J. Am. Chem. Soc.* **1971**, *93*, 6174–6181. (c) Kresge, A. J.; Mylonakis, S. G.; Sato, Y.; Vitullo, V. P. *J. Am. Chem. Soc.* **1971**, *93*, 6181–6188.

(19) Minegishi, S.; Loos, R.; Kobayashi, S.; Mayr, H. *J. Am. Chem. Soc.* **2005**, *127*, 2641–2649.

(20) Streidl, N.; Denegri, B.; Kronja, O.; Mayr, H. *Acc. Chem. Res.* **2010**, *43*, 1537–1549.

(21) Schaller, H. F.; Tishkov, A. A.; Feng, X.; Mayr, H. *J. Am. Chem. Soc.* **2008**, *130*, 3012–3022.

(22) (a) Richard, J. P. *Tetrahedron* **1995**, *51*, 1535–1573. (b) Richard, J. P.; Amyes, T. L.; Williams, K. B. *Pure Appl. Chem.* **1998**, *70*, 2007–

2014. (c) Amyes, T. L.; Stevens, I. W.; Richard, J. P. *J. Org. Chem.* **1993**, *58*, 6057–6066. (d) Amyes, T. L.; Richard, J. P. *J. Chem. Soc., Chem. Commun.* **1991**, 200–202. (e) Richard, J. P. *J. Am. Chem. Soc.* **1989**, *111*, 1455–1465.

(23) For details on Marcus theory, see: (a) Marcus, R. A. *Annu. Rev. Phys. Chem.* **1964**, *15*, 155–196. (b) Marcus, R. A. *J. Phys. Chem.* **1968**, *72*, 891–899. (c) Marcus, R. A. *J. Am. Chem. Soc.* **1969**, *91*, 7224–7225. (d) Albery, W. J.; Kreevoy, M. M. *Adv. Phys. Org. Chem.* **1978**, *16*, 87–157. (e) Albery, W. J. *Annu. Rev. Phys. Chem.* **1980**, *31*, 227–263. (f) Marcus, R. A. *Pure Appl. Chem.* **1997**, *69*, 13–29. (g) Marcus, R. A. *Angew. Chem.* **1993**, *105*, 1161–1172; *Angew. Chem., Int. Ed. Engl.* **1993**, *32*, 1111–1121. (h) Peters, K. S.; Gasparrini, S.; Heeb, L. R. *J. Am. Chem. Soc.* **2005**, *127*, 13039–13047.

(24) Mayr, H.; Bug, T.; Gotta, M. F.; Hering, N.; Irrgang, B.; Janker, B.; Kempf, B.; Loos, R.; Ofial, A. R.; Remennikov, G.; Schimmel, H. *J. Am. Chem. Soc.* **2001**, *123*, 9500–9512.

(25) *Vinyl Cations*; Stang, P., Rappoport, Z., Hanack, M., Subramanian, L. R., Eds.; Academic Press: New York, 1979.

(26) (a) *Dicoordinated Cations*; Rappoport, Z., Stang, P. J., Eds.; Wiley: New York, 1997. (b) Grob, C. A. *Dicoordinated Cations*; Wiley: New York, 1997; Chapter 1, pp 1–7. (c) Stang, P. J. In *Prog. Phys. Org. Chem.*; Streitwieser, A. J., Jr., Taft, R. W., Eds.; Wiley and Sons: New York, 1973; Vol. 10, pp 205–325. (d) Rappoport, Z. In *Reactive Intermediates*; Abramovitch, R. A., Ed.; Plenum Press: New York, 1983; Vol. 3, pp 427–615. (e) Modena, G.; Tonellato, U. *Adv. Phys. Org. Chem.* **1971**, *9*, 185–280.

(27) Kitamura, T.; Taniguchi, H. In *Dicoordinated Cations*; Rappoport, Z., Stang, P. J., Eds.; Wiley: New York, 1997; Chapter 7, pp 321–376.

(28) Generation of β -silyl-substituted vinyl cations that are stable at low temperature in superacidic media: (a) Siehl, H.-U.; Kaufmann, F.-P.; Apeloig, Y.; Braude, V.; Danovich, D.; Berndt, A.; Stamatias, N. *Angew. Chem.* **1991**, *103*, 1546–1549; *Angew. Chem., Int. Ed. Engl.* **1991**, *30*, 1479–1482. (b) Siehl, H.-U.; Müller, T.; Gauss, J.; Buzek, P.; Schleyer, P. v. R. *J. Am. Chem. Soc.* **1994**, *116*, 6384–6387. (c) Kaufmann, F.-P.; Siehl, H.-U. *J. Am. Chem. Soc.* **1992**, *114*, 4937–4939. (d) Siehl, H.-U.; Kaufmann, F.-P.; Hori, K. *J. Am. Chem. Soc.* **1992**, *114*, 9343–9349.

(29) Generation of room temperature-stable silyl-substituted vinyl cations: (a) Klaer, A.; Syha, Y.; Nasiri, H. R.; Müller, T. *Chem. - Eur. J.* **2009**, *15*, 8414–8423. (b) Müller, T.; Meyer, R.; Lennartz, D.; Siehl, H.-U. *Angew. Chem.* **2000**, *112*, 3203–3206; *Angew. Chem., Int. Ed.* **2000**, *39*, 3074–3077. (c) Müller, T.; Margraf, D.; Syha, Y. *J. Am. Chem. Soc.* **2005**, *127*, 10852–10860. (d) Müller, T.; Juhasz, M.; Reed, C. A. *Angew. Chem.* **2004**, *116*, 1569–1572; *Angew. Chem., Int. Ed.* **2004**, *43*, 1543–1546.

(30) Aue, D. H. In *Dicoordinated Carbocations*; Rappoport, Z., Stang, P. J., Eds.; Wiley: New York, 1997; pp 105–156. In particular, see pp 126–129, Table 2.

(31) Calculations on stabilities of vinyl cations: (a) Apeloig, Y.; Franke, W.; Rappoport, Z.; Schwarz, H.; Stahl, D. *J. Am. Chem. Soc.* **1981**, *103*, 2770–2780. (b) Apeloig, Y.; Schleyer, P. v. R.; Pople, J. A. *J. Am. Chem. Soc.* **1977**, *99*, 1291–1296. (c) Apeloig, Y.; Schleyer, P. v. R.; Pople, J. A. *J. Org. Chem.* **1977**, *42*, 3004–3011. (d) Apeloig, Y.; Schleyer, P. v. R.; Pople, J. A. *J. Am. Chem. Soc.* **1977**, *99*, 5901–5909. (e) Apeloig, Y.; Stanger, A. *J. Org. Chem.* **1982**, *47*, 1462–1468. (f) van Alem, K.; Lodder, G.; Zuillhof, H. *J. Phys. Chem. A* **2002**, *106*, 10681–10690. (g) Alem, K.; Lodder, G.; Zuillhof, H. *J. Phys. Chem. A* **2000**, *104*, 2780–2787. (h) Mayr, H.; Schneider, R.; Wilhelm, D.; Schleyer, P. v. R. *J. Org. Chem.* **1981**, *46*, 5336–5340.

(32) Studies of the stabilities of vinyl cations $[\text{ArC}=\text{CH}_2]^+$ by ion cyclotron resonance techniques: (a) Kobayashi, S.; Matsumoto, T.; Taniguchi, H.; Mishima, M.; Fujio, M.; Tsuno, Y. *Tetrahedron Lett.* **1993**, *34*, 5903–5906. (b) Mishima, M.; Ariga, T.; Fujio, M.; Tsuno, Y.; Kobayashi, S.; Taniguchi, H. *Chem. Lett.* **1992**, *21*, 1085–1088.

(33) Cozens, F. L.; Kanagasabapathy, V. M.; McClelland, R. A.; Steenken, S. *Can. J. Chem.* **1999**, *77*, 2069–2082.

(34) (a) Kobayashi, S.; Hori, Y.; Hasako, T.; Koga, K.; Yamataka, H. *J. Org. Chem.* **1996**, *61*, 5274–5279. (b) Kobayashi, S.; Schnabel, W. Z.

- Naturforsch., B: J. Chem. Sci.* **1992**, *47*, 1319–1323. (c) Kobayashi, S.; Zhu, Q. Q.; Schnabel, W. Z. *Naturforsch., B: J. Chem. Sci.* **1988**, *47*, 825–829.
- (35) Ammer, J.; Nolte, C.; Mayr, H. *J. Am. Chem. Soc.* **2012**, *134*, 13902–13911.
- (36) Nigst, T.; Westermaier, M.; Ofial, A. R.; Mayr, H. *Eur. J. Org. Chem.* **2008**, 2369–2374.
- (37) Kanzian, T.; Nigst, T. A.; Maier, A.; Pichl, S.; Mayr, H. *Eur. J. Org. Chem.* **2009**, 6379–6385.
- (38) Minegishi, S.; Kobayashi, S.; Mayr, H. *J. Am. Chem. Soc.* **2004**, *126*, 5174–5181.
- (39) (a) Rappoport, Z.; Kaspi, J. *J. Am. Chem. Soc.* **1974**, *96*, 4518–4530. (b) Rappoport, Z.; Kaspi, J. *J. Am. Chem. Soc.* **1970**, *92*, 3220–3221. (c) Rappoport, Z.; Apeloig, Y. *J. Am. Chem. Soc.* **1969**, *91*, 6734–6742. (d) Rappoport, Z.; Gal, A. *J. Am. Chem. Soc.* **1969**, *91*, 5246–5254.
- (40) (a) Rappoport, Z.; Kaspi, J. *J. Chem. Soc., Perkin Trans. 2* **1972**, 1102–1111. (b) Miller, L. L.; Kaufman, D. A. *J. Am. Chem. Soc.* **1968**, *90*, 7282–7287. (c) Rappoport, Z.; Gal, A. *J. Chem. Soc., Perkin Trans. 2* **1973**, 301–310.
- (41) (a) Rappoport, Z.; Kaspi, J. *J. Am. Chem. Soc.* **1975**, *97*, 821–835. (b) Rappoport, Z.; Kaspi, J. *J. Am. Chem. Soc.* **1974**, *96*, 586–588.
- (42) Hofmann, M.; Hampel, N.; Kanzian, T.; Mayr, H. *Angew. Chem.* **2004**, *116*, 5518–5521; *Angew. Chem., Int. Ed.* **2004**, *43*, 5402–5405.
- (43) No side products were formed; that is, other than the 3-vinylpyrrole products, only starting materials remained when the reaction was stopped.
- (44) *ipso*-Substitution with cyanide: Kitamura, T.; Murakami, M.; Kobayashi, S.; Taniguchi, H. *Tetrahedron Lett.* **1986**, *27*, 3885–3888.
- (45) *ipso*-Substitution with alkoxide: (a) Kitamura, T.; Kabashima, T.; Kobayashi, S.; Taniguchi, H. *Tetrahedron Lett.* **1988**, *29*, 6141–6142. (b) Kitamura, T.; Nakamura, I.; Kabashima, T.; Kobayashi, S.; Taniguchi, H. *Chem. Lett.* **1990**, *19*, 9–12. (c) Kitamura, T.; Nakamura, I.; Kabashima, T.; Kobayashi, S.; Taniguchi, H. *J. Am. Chem. Soc.* **1990**, *112*, 6149–6150. (d) Kitamura, T.; Kabashima, T.; Nakamura, I.; Fukada, T.; Taniguchi, H. *J. Am. Chem. Soc.* **1991**, *113*, 7255–7261. (e) Kitamura, T.; Kabashima, T.; Kobayashi, S.; Taniguchi, H. *Chem. Lett.* **1988**, *17*, 1951–1954. (f) Kitamura, T.; Nakamura, I.; Kabashima, T.; Kobayashi, S.; Taniguchi, H. *J. Chem. Soc., Chem. Commun.* **1989**, 0, 1154–1155. (g) Kitamura, T.; Soda, S.; Nakamura, I.; Fukada, T.; Taniguchi, H. *Chem. Lett.* **1991**, *20*, 2195–2198. (h) Hori, K.; Kamada, H.; Kitamura, T.; Kobayashi, S.; Taniguchi, H. *J. Chem. Soc., Perkin Trans. 2* **1992**, 871–877.
- (46) Interception with azide and cyanate nucleophiles: (a) Kitamura, T.; Kobayashi, S.; Taniguchi, H. *Tetrahedron Lett.* **1979**, *20*, 1619–1622. (b) Kitamura, T.; Kobayashi, S.; Taniguchi, H. *J. Org. Chem.* **1984**, *49*, 4755–4760.
- (47) Interception with thiocyanate: (a) Kitamura, T.; Kobayashi, S.; Taniguchi, H. *Chem. Lett.* **1984**, *13*, 1523–1526. (b) Kitamura, T.; Kobayashi, S.; Taniguchi, H. *J. Org. Chem.* **1990**, *55*, 1801–1805.
- (48) Interception with acetate or bromide (labeled): van Ginkel, F. I. M.; Cornelisse, J.; Lodder, G. *J. Am. Chem. Soc.* **1991**, *113*, 4261–4272.
- (49) Interception with methylphenylsulfide: Kitamura, T.; Kabashima, T.; Taniguchi, H. *J. Org. Chem.* **1991**, *56*, 3739–3741.
- (50) The transient UV–vis spectra of **2** and **3** are included on p S45 of the Supporting Information.
- (51) The decay curves for the reactions of **2** with nucleophiles **7–9** and **11** ceased to be monoexponential once a certain conversion had been reached. The use of a particularly large excess of the nucleophile was necessary in each case (involving **7–9** and **11**) to produce decay curves in which the first 50–80% of the decay was monoexponential (i.e., to overcome the influence of background reactions). In reactions of **3** with **7–9**, the observed rate constants for the decays of the vinyl cations never exceeded the rate of the reaction of the solvent with **3**. We discuss this material in greater detail in the Supporting Information on pp S40–42.
- (52) McClelland, R. A.; Kanagasabapathy, V. M.; Banait, N. S.; Steenken, S. *J. Am. Chem. Soc.* **1989**, *111*, 3966–3972.
- (53) (a) Lucius, R.; Loos, R.; Mayr, H. *Angew. Chem.* **2002**, *114*, 97–102; *Angew. Chem., Int. Ed.* **2002**, *41*, 91–95. (b) Mayr, H. *Tetrahedron* **2015**, *71*, 5095–5111.
- (54) Phan, T. B.; Breugst, M.; Mayr, H. *Angew. Chem.* **2006**, *118*, 3954–3959; *Angew. Chem., Int. Ed.* **2006**, *45*, 3869–3874.
- (55) Experimentally determined rate constants were used where available; otherwise $\lg k(47)$ was calculated using eq 4, using $E = 0.00$ (for **47**)²⁴ and the relevant N and s_N values from Table 1. Calculated rate constants for nucleophiles **17–20** exceed the diffusion limit, and hence are not included in the correlation.
- (56) Experimentally determined rate constants were used where available; otherwise $\lg k(48)$ was calculated using eq 4, using $E = 3.63$ (for **48**)³⁵ and the relevant N and s_N values from Table 2. Pyrrole **10** is not included in the correlation because the rate constant calculated for its reaction with **48** greatly exceeds the diffusion limit. The absence of this number undoubtedly contributes to the apparent better quality of the correlation in Figure 9 as compared to Figure 8.
- (57) Liu, K.-T.; Chin, C.-P.; Lin, Y.-S.; Tsao, M.-L. *Tetrahedron Lett.* **1995**, *36*, 6919–6922.
- (58) McClelland, R. A.; Kanagasabapathy, V. M.; Steenken, S. *J. Am. Chem. Soc.* **1988**, *110*, 6913–6914.
- (59) (a) Hojo, M.; Ueda, T.; Ueno, E.; Hamasaki, T.; Nakano, T. *Bull. Chem. Soc. Jpn.* **2010**, *83*, 401–414. (b) Hojo, M.; Aoki, S. *Bull. Chem. Soc. Jpn.* **2012**, *85*, 1023–1030. (c) Manege, L. C.; Ueda, T.; Hojo, M.; Fujio, M. *J. Chem. Soc., Perkin Trans. 2* **1998**, 1961–1966.
- (60) (a) See p 483 in ref 1d. (b) See ref 2S, pp 290–447, and in particular pp 355–391. (c) See ref 26d, pp 583–594.
- (61) See ref 2S, p 361, Table 6.2S.
- (62) Frisch, M. J.; Trucks, G. W.; Schlegel, H. B.; Scuseria, G. E.; Robb, M. A.; Cheeseman, J. R.; Scalmani, G.; Barone, V.; Mennucci, B.; Petersson, G. A.; Nakatsuji, H.; Caricato, M.; Li, X.; Hratchian, H. P.; Izmaylov, A. F.; Bloino, J.; Zheng, G.; Sonnenberg, J. L.; Hada, M.; Ehara, M.; Toyota, K.; Fukuda, R.; Hasegawa, J.; Ishida, M.; Nakajima, T.; Honda, Y.; Kitao, O.; Nakai, H.; Vreven, T.; Montgomery, J. A., Jr.; Peralta, J. E.; Ogliaro, F.; Bearpark, M.; Heyd, J. J.; Brothers, E.; Kudin, K. N.; Staroverov, V. N.; Kobayashi, R.; Normand, J.; Raghavachari, K.; Rendell, A.; Burant, J. C.; Iyengar, S. S.; Tomasi, J.; Cossi, M.; Rega, N.; Millam, M. J.; Klene, M.; Knox, J. E.; Cross, J. B.; Bakken, V.; Adamo, C.; Jaramillo, J.; Gomperts, R.; Stratmann, R. E.; Yazyev, O.; Austin, A. J.; Cammi, R.; Pomelli, C.; Ochterski, J. W.; Martin, R. L.; Morokuma, K.; Zakrzewski, V. G.; Voth, G. A.; Salvador, P.; Dannenberg, J. J.; Dapprich, S.; Daniels, A. D.; Farkas, Ö.; Foresman, J. B.; Ortiz, J. V.; Cioslowski, J.; Fox, D. J. *Gaussian 09*, revision D.01; Gaussian, Inc.: Wallingford, CT, 2009.
- (63) See Supporting Information pp S54–S59 for details of the calculations.
- (64) (a) Becke, A. D. *J. Chem. Phys.* **1993**, *98*, 5648–5652. (b) Lee, C.; Yang, W.; Parr, R. G. *Phys. Rev. B: Condens. Matter Mater. Phys.* **1988**, *37*, 785–789.
- (65) As no barrier between the vinyl bromide **4-Br** and the ion pair $\{2\}Br^-$ is found using the PCM method (see Figure 11), the ΔG° values given in entries 6 and 8 correspond to solvolysis half-lives on the micro- and millisecond time scale, in sharp contrast to the experimental finding that **4-Br** solvolyzes with a half-life of 1 year in 80% aqueous ethanol at 25 °C (Scheme 4).
- (66) Tao, J. M.; Perdew, J. P.; Staroverov, V. N.; Scuseria, G. E. *Phys. Rev. Lett.* **2003**, *91*, 146401.
- (67) (a) Grimme, S.; Antony, J.; Ehrlich, S.; Krieg, H. *J. Chem. Phys.* **2010**, *132*, 154104. (b) Grimme, S.; Hansen, A.; Brandenburg, J. G.; Bannwarth, C. *Chem. Rev.* **2016**, *116*, 5105–5154.
- (68) Tomasi, J.; Mennucci, B.; Cammi, R. *Chem. Rev.* **2005**, *105*, 2999–3093.
- (69) Plata, R. E.; Singleton, D. A. *J. Am. Chem. Soc.* **2015**, *137*, 3811–3826.
- (70) See Supporting Information pp S60–75 for details of the calculations of the hydride affinities and analysis of the hydrido-bridged species at different levels of theory.
- (71) For previous experimental and theoretical investigations of hydride affinities of carbocations, see refs 4 and 5.